Published in final edited form as:
Nanomedicine (Lond). 2013 November ; 8(11): . doi:10.2217/nnm.12.204.

Poly(ε-caprolactone)-carbon nanotube composite scaffolds for enhanced cardiac differentiation of human mesenchymal stem cells

Spencer W Crowder[1,2], **Yi Liang**[1], **Rutwik Rath**[1,2], **Andrew M Park**[3], **Simon Maltais**[4], **Peter N Pintauro**[3], **William Hofmeister**[5], **Chee C Lim**[6], **Xintong Wang**[1,2], and **Hak-Joon Sung**[1,2,6,*]

[1]Department of Biomedical Engineering, Vanderbilt University, Nashville, TN, USA

[2]Center for Stem Cell Biology, Vanderbilt University Medical Center, Nashville, TN, USA

[3]Department of Chemical & Biomolecular Engineering, Vanderbilt University, Nashville, TN, USA

[4]Department of Cardiac Surgery & Cardiology, Vanderbilt University Medical Center, Nashville, TN, USA

[5]Center for Laser Applications, University of Tennessee Space Institute, Tullahoma, TN, USA

[6]Department of Medicine, Cardiovascular Medicine, Vanderbilt University Medical Center, Nashville, TN, USA

Abstract

Aim—To evaluate the efficacy of electrically conductive, biocompatible composite scaffolds in modulating the cardiomyogenic differentiation of human mesenchymal stem cells (hMSCs).

Materials & methods—Electrospun scaffolds of poly(ε-caprolactone) with or without carbon nanotubes were developed to promote the *in vitro* cardiac differentiation of hMSCs.

Results—Results indicate that hMSC differentiation can be enhanced by either culturing in electrically conductive, carbon nanotube-containing composite scaffolds without electrical stimulation in the presence of 5-azacytidine, or extrinsic electrical stimulation in nonconductive poly(ε-caprolactone) scaffolds without carbon nanotube and azacytidine.

Conclusion—This study suggests a first step towards improving hMSC cardiomyogenic differentiation for local delivery into the infarcted myocardium.

*Author for correspondence: Tel.: +1 615 322 6986, Fax: +1 615 343 7919, hak-joon.sung@vanderbilt.edu.

Ethical conduct of research

The authors state that they have obtained appropriate institutional review board approval or have followed the principles outlined in the Declaration of Helsinki for all human or animal experimental investigations. In addition, for investigations involving human subjects, informed consent has been obtained from the participants involved.

Financial & competing interests disclosure

Confocal imaging was performed through the use of the Vanderbilt University Medical Center Cell Imaging Shared Resource (supported by NIH grants CA68485, DK20593, DK58404, HD15052, DK59637 and EY08126). This work was directly supported by the NIH (NIH HL091465), the National Science Foundation (CAREER: CBET 1056046) and Vanderbilt Start-up. The authors have no other relevant affiliations or financial involvement with any organization or entity with a financial interest in or financial conflict with the subject matter or materials discussed in the manuscript apart from those disclosed.

No writing assistance was utilized in the production of this manuscript.

Keywords

carbon nanotube; cardiac differentiation; electrical conductivity; mesenchymal stem cell; poly(ε-caprolactone)

The ability of distinctive characteristics in nanomaterials to modulate cell behavior has received increasing interest in the last several years. These characteristics include mechanical [1], chemical [2], electrical [3–5] and topographical [6] properties, and can be tailored to intricately control cell function and phenotype in order to enhance consequent therapeutic outcomes; in particular, from stem cell populations that possess the ability to differentiate into various cell types. By mimicking the microenvironmental cues that either stimulate cell type-specific differentiation of stem cells [7,8] or maintain physiological function of either progenitor or terminally differentiated cells [3,5], novel nanomaterial-based schemes can be developed to improve the efficacy of clinically translatable cell-based therapies.

Myocardial infarction with resultant congestive heart failure is a leading cause of death in the western world due to a limited ability of the myocardium to regenerate lost or damaged tissue after injury [9]. Currently, heart transplantation is the primary treatment option for end-stage heart failure, but the limited number of donors cannot meet the high level of patient demand, indicating a critical need for developing novel cell-based cardiac therapies [10]. Human mesenchymal stem cells (hMSCs) are an adult-derived cell source with multilineage differentiation potential, immunomodulatory capabilities and can be used in an 'off-the-shelf,' allogenic manner [11]. *In vivo* models of myocardial infarction have revealed that rat MSCs home to and integrate at the infarcted site and participate in postinfarction angiogenesis [12], suggesting that MSCs intrinsically possess therapeutic functions for cardiac regeneration and repair. Interestingly, *in vitro* cocultures of MSCs with cardiomyocytes resulted in differentiation towards a cardiomyogenic lineage through Notch-mediated signaling [13]. In parallel, short-term treatment with the nonspecific DNA methylation inhibitor 5-azacytidine (Aza) has also been shown to stimulate *in vitro* cardiomyogenesis in both rat [14] and human [15] MSCs. hMSCs have been investigated extensively in a number of clinical trials for cardiac therapy, yet significant work remains before the clinical relevance of hMSCs is realized [9,16]. Specifically, direct cardiac injection of autologous, naive hMSCs in human patients suffering from chronic heart failure was shown to yield no significant improvement in cardiac function, suggesting that additional stimuli may be required to elucidate the therapeutic effect of hMSCs [17].

Cardiac tissue relies heavily upon electrical signaling for cooperative contraction and cell–cell communication. Electrically conductive substrates might play a key role in enhancing cardiomyogenic differentiation of hMSCs [10]. hMSCs have been shown to uptake electrically conductive carbon nanotubes (CNTs) without affecting cell viability, proliferation or differentiation capacity [18]. CNT-based culture substrates have been employed in a number of studies related to the maintenance or *de novo* formation of cardiac tissue, including maturation of cardiomyocyte precursors [3], injectable polymer/CNT composites for enhancing cardiomyocyte proliferation and function [19], and cardiac differentiation of stem cells [20]. Through the use of well-defined engineering systems, the findings from these studies have indicated that CNTs, electrical conductivity and/or electrical stimulation (ES) play a role in encouraging or modulating cardiac function; however, unlike some of the approaches to date, the electrospinning procedure presented here, as well as the materials used in this study, lend themselves to scalability at a low cost, which is a requisite for technologies to eventually see clinical translation. In addition, the strategy employed in this study combines material- and biochemical-mediated approaches to

identify synergistic relationships for enhancing cardiac differentiation of hMSCs. Poly(ε-caprolactone) (PCL) is a commonly used nonconducting, biocompatible polymer that has been studied extensively for tissue-engineering applications [21], including cardiomyogenic differentiation of murine embryonic stem cells [22]. Since CNTs and PCL offer complimentary properties, combining the two materials to develop an electrically conductive, biocompatible culture substrate for enhanced cardiomyogenic differentiation of hMSCs provides an ideal framework for improving clinically relevant cardiac regeneration. In parallel, concurrent biochemical treatment with known inducers of cardiac differentiation, such as the Notch signaling protein Jagged 1 (Jag) [13] or an inducer of epigenetic alteration, Aza [14,15], during culture on electrically active substrates could further enhance the differentiation.

In the present study, we developed electrically conductive composite scaffolds of electrospun PCL embedded with CNTs as synthetic, 3D hMSC culture substrates. We first characterized the role of organic solvent selection in controlling the uniform distribution of CNTs in electrospun fibers, and then identified the optimal loading concentration of CNTs for enhanced electrical conductivity. We cultured hMSCs in these scaffolds in the presence of either Aza or Jag with and without extrinsic ES. We found:

- CNT-containing scaffolds possess an inherent ability to promote a cardiomyocyte-like morphology of hMSCs (i.e., elongated and rod-shaped) even in 3D culture;
- Treatment of hMSCs with Aza on CNT-containing substrates further stimulates upregulation of cardiac-related markers at the gene level and colocalization of contractile proteins at the whole-cell level;
- Extrinsic ES can have divergent effects on hMSC differentiation, depending upon the substrate conductivity. These findings are applicable to the fields of nanomedicine and will be used to design a multifaceted approach for improving cardiomyogenic differentiation of hMSCs in a clinically translatable manner.

Materials & methods

Chemicals, reagents & CNTs

PCL was synthesized by the ring-opening polymerization of ε-caprolactone (Alfa Aesar, MA, USA) as previously described [22,23], with an average molecular weight of 90–100 kDa as determined by gel permeation chromatography. Tetrahydrofuran (THF), dichlorobenzene (DCB) and dimethylformamide (DMF) were purchased from Sigma-Aldrich (MO, USA) and used as received. Multiwall CNTs (MWCNTs) were synthesized in an ASTeX Large Area Diamond Deposition System (Seki Technotron Corp., Tokyo, Japan) as a byproduct of diamond synthesis. The synthesis chamber is a root blower recirculated plasma torch chemical vapor deposition chamber run at 800°C sample temperature in a gas mixture at 60 torr (H_2: 700 standard cm^3/min [SCCM]; CH_4: 100 SCCM; and CO_2: 40 SCCM).

Electrospinning procedure

MWCNTs stock solutions (2–4% w/v) were prepared in THF or DCB, and sonicated for 4 h to ensure MWCNT dispersion. PCL solutions (15% w/v) were prepared in a 1:1 v/v mixture of either THF:DMF, THF:DCB or DCB:DMF with or without the appropriate volume of MWCNT stock solution. Test groups included 0, 1, 3, 5 and 10% w/w MWCNT/polymer. The polymer and MWCNT solutions were subsequently vortexed for 1 h to ensure proper mixing.

For electrospinning, polymer/MWCNT solutions were drawn into a glass syringe (10 ml) attached with a stainless steel needle (22 G) with a smooth tip. All electrospinning was performed at room temperature and humidity (20–30%). An alligator clip connected to a tunable, high-voltage power supply was attached to the tip of the needle (positive lead) with the negative lead connected to a grounded cylindrical mandrel. The PCL solutions were ejected at a flow rate of 1 ml/h using a syringe pump. The voltage used for electrospinning was 15 kv and the needle-to-collector distance was 10 cm. The rotation speed of the mandrel was 1500 rpm. For material characterization, polymer mats were spun directly onto the rotating mandrel for 20 min. For cell studies, a thin layer of plasma-treated poly(dimethyl siloxane) (PDMS, Sylgard 184, Superior Essex, GA, USA) was wrapped around the mandrel and mats were spun on top of the PDMS for 4 h. Subsequently, 15-mm circles were punched out of the mat, left under vacuum overnight to remove excess solvent, sterilized under UV light for 30 min per side, and placed into 24-well plates for cell culture studies. The PDMS layer served two purposes: to act as a sturdy backing material to handle the mats during cell culture, and to prevent the mats from floating freely in the culture media.

Scanning & transmission electron microscopy

For scanning electron microscopy, fibers were collected for 20 min over an aluminum woven mesh with a wire diameter of 1.0 mm and a wire spacing of 0.381 mm (McMaster-Carr Co., NJ, USA) that was attached to the rotating mandrel. Meshes were coated with gold using a sputter coater (Cressington Scientific, Watford, UK) for 2 min at a separation height of 12 cm. The fibers were examined using a scanning electron microscope (Hitachi S-4200, Tokyo, Japan) at an accelerating voltage of 1–5 kv.

Transmission electron microscope (TEM) copper-mesh imaging grids (Ted Pella Inc., CA, USA) were placed onto PDMS squares and attached to the rotating mandrel for direct deposition of electrospun mats. PDMS was used to avoid damaging the TEM grid. After spinning, mats were vacuum-dried for 24 h. Transmission electron microscopy was performed with a Philips CM20 TEM (EO, The Netherlands) to confirm presence of MWCNTs within the polymer fibers and to determine their diameter. A total of 1 μl of MWCNT stock solutions with THF or DCB was deposited onto the TEM grid and vacuum-dried for 24 h to prepare the controls.

Mechanical analysis

Electrospun samples were cut into rectangular strips with a thickness of 500–600 μm. The width and thickness of each mat varied between samples and was measured at least four-times along the sample length to ensure accurate calculations of stress and strain. Mechanical analysis was performed with an Enduratec Electroforce 3100 mechanical tester (Bose Corporation, MN, USA) with a preload force of 0.03 N and an initial separation distance of 2.25 mm. Samples were stretched at a rate of 0.1 mm s^{-1} until failure. A force/displacement curve was generated from the data, which was then converted to stress/strain by normalizing to the relevant dimensions, and the elastic modulus was calculated by measuring the slope of the linear portion of the stress/strain curve (n = 9 samples/group).

Electrical conductivity measurements

The in-plane conductivity of the fiber mats was measured by electrochemical impedance spectroscopy using a Gamry potentiostat and a four-probe Bekktech conductivity cell (Scribner Associates Inc., NC, USA). Data were collected at room temperature in deionized water following incubation in dH_2O overnight to represent physiologically relevant, aqueous conditions. Conductivity was calculated using Equation 1:

$$\sigma = \frac{L}{w \times \delta \times R} \quad (1)$$

where σ = conductivity (mS cm^{-1}); L = distance between the two working electrodes (cm); w = width of the membrane sample (cm); δ = membrane thickness (cm); and R is the calculated ionic resistance (Ω). Both δ and w are wet-state dimensions (n = 3 samples/group). Conductivity values were normalized to the volume fraction occupied by polymer fibers, ranging from 82 to 86% of total volume, calculated using the fiber mat dimensions and the known density of PCL (1.145 g/cm^3). For this calculation, the density of CNTs was assumed to be negligible in comparison to that of PCL. Pure PCL mats showed no appreciable conductivity and therefore a conductivity value for control samples was not listed.

Differential scanning calorimetry

Differential scanning calorimetry (Q1000, TA Instruments, DE, USA) was performed with a sample mass between 5 and 10 mg in aluminum pans with tops. The procedure included two temperature sweeps from −80 to 100°C at a ramp rate of 10°C/min, and the curves from the first sweep are reported such that the characteristics of intact electrospun fibers were accurately demonstrated. Data were analyzed and graphed with Universal Analysis software (TA Instruments).

Cell culture & immunocytochemistry

hMSCs (passages 4–6) were maintained in DMEM, Gibco® Cell Culture (Invitrogen, CA, USA), supplemented with 10% MSC-qualified fetal bovine serum (Gibco) with 1% penicillin– streptomycin (Gibco) at 37°C and 5% CO_2. Polymer scaffolds were coated with 0.2% sterilefiltered gelatin (Sigma-Aldrich) overnight at 37°C to improve cell attachment. hMSCs were seeded at a density of 5000 cells/cm^2 for all experiments. To trigger cardiomyogenic differentiation, cells were treated with either Jag (5 μg/ml, R&D Systems, MN, USA) [13] or Aza (10 μM, Sigma-Aldrich) [14]. Cells were seeded on tissue culture polystyrene (TCPS), PCL or PCL with CNTs, allowed to attach overnight in DMEM, and the media was then changed to DMEM with or without chemical treatment for 3 days. Cells were then propagated (with/without ES) for an additional 4 days in media without chemical treatment before end point evaluations (8 day total culture). ES was performed with a C-Pace cell culture pacing system (Ion Optix, MA, USA) for 10 min per day for 4 days using the following parameters: 500 v/m and 5 ms pulse width at 1 Hz.

For immunocytochemistry, cells were fixed with 4% paraformaldehyde for 15 min, permeabilized with 0.25% Triton X in phosphate-buffered saline for 10 min, and blocked with 10% goat serum in phosphate-buffered saline. Unless otherwise stated, all steps were performed at room temperature. Cells were then incubated with 1:100 mouse antihuman myosin heavy chain (MYH), followed by 1:200 DyLight488- conjugated goat antimouse (Abcam, MA, USA), each for 1 h. Cells were then incubated with Texas Red-X-conjugated phalloidin (Molecular Probes, CA, USA) for 20 min according to the manufacturer's instructions, and nuclei were counterstained with Hoechst (Sigma-Aldrich). Cells were imaged with a LSM 710 META Inverted Confocal Microscope (Carl Zeiss, LLC, NY, USA), and postprocessed and analyzed with Image J (NIH, MD, USA).

Reverse transcriptase PCR

RNA was harvested with the Trizol reagent (Invitrogen) following the manufacturer's protocol, and RNA 'clean up' was performed with the RNeasy kit (Qiagen, CA, USA). cDNA was synthesized using the iScript cDNA synthesis kit (Bio-Rad, CA, USA). RT-PCR

was performed using the iQ SYBR Green supermix (Bio-Rad) on a Bio-Rad CFX Real Time Instrument with n ≥ 3 technical replicates for the following genes: *GAPDH*, α-*MYH*, *RYR2*, *Nkx2.5* and *cTNT*. Primer sequences were: GAPDH 5′-GCC TCA AGA TCA TCA GCA ATG-3′ (sense) and 5′-CTT CCA CGA TAC CAA AGT TGTC-3′(antisense); α-MHC 5′-ACT CCT GCG GCC CAG ATT CTT-3′ (sense) and 5′-GCG AAT GTC AAA GGG CCG GGT- 3′ (antisense); RYR2 5′-CTG CCA AGG CAT CGG GCT GT-3′ (sense) and 5′-CAT CTC AGC CGC GCC ACG AT-3′ (antisense); Nkx2.5 5′-AGT GCT CTG CTC AGA CAG CCC AG-3′ (sense) and 5′-GGC CCT TCC CCC TCC TCC ATA-3′ (antisense); and cTNT 5′-AGC CCA GGT CGT TCA TGC CC-3′(sense) and 5′-ATT CCG GAT GCG CTG CTG CT-3′ (antisense). Data were analyzed with CFX Manager software (Bio-Rad) and results were presented as ΔΔC(t) expression normalized to GAPDH. In Figure 4, expression values were further normalized to TCPS no treatment sample as a control since this is the general standard by which hMSCs are cultured. In contrast, there was not a sample control for the data listed in Figure 6 because TCPS was not used for this section of the study.

Statistical analysis

In all experiments, results are presented as a mean ± standard error of the mean. Results from each experiment were initially analyzed using single factor analysis of variance and comparisons between individual sample groups were then performed using an unpaired Student's *t*-test. For all statistics, $p < 0.05$ was considered statistically significant.

Results & discussion

Solvent selection

Fiber size and uniformity are of great importance for accurately elucidating cellular responses because cells sense and adapt to local changes in their physical micro-/nano-environment [6,24]. Identifying the best solvent mixture for electrospinning uniform fibers containing both PCL and CNTs was therefore a high priority. Three solvents were studied first to control fiber size and uniformity. THF effectively solubilizes PCL [21] and has a low boiling point, whereas DMF has a high boiling point and has been used in similar studies [25]. DCB was also tested because it acts as a surfactant to improve dispersion of CNTs in solution [26]. We analyzed the resulting fibers without CNTs (control) and with 1% CNTs in order to gain initial insight into how CNTs affect fiber properties.

Fibers spun in THF/DMF did not form beads, but fibers spun in either THF/DCB or DCB/DMF formed a large amount of beads (Figures 1A–1D). The THF/DMF solvent group produced the largest fibers (~2.5 μm), whereas THF/DCB and DCB/DMF groups produced much smaller fibers (~0.3–0.5 μm, Figures 1B–1D). Fiber diameter decreased significantly upon addition of 1% CNT in the THF/DMF and THF/DCB solvent groups, but increased in the DCB/DMF solvent group. Control fibers (i.e., PCL without CNTs) for each solvent group exhibited an elastic modulus within a similar range (~15–17 MPa), and the inclusion of 1% CNTs caused an increase in modulus for all groups (Figure 1C). Moving forward, we chose the THF/DMF solvent group because large, uniform fibers could be produced without bead formation, providing a reproducible means for studying the effects of CNTs on fiber mat properties, as well as the resulting cellular response.

CNT loading optimization

We then investigated how the CNT loading concentration affected fiber mat properties. Fiber mats containing 0, 1, 3, 5 and 10% CNTs were evaluated in terms of fiber diameter, elastic modulus, conductivity and thermal properties (Figures 2 & 3). Increasing CNT concentration resulted in smaller fibers, but overall the mats became stiffer (Figures 2A–2B), similar to what was previously reported by Saeed *et al.* [27]. Qualitatively, the fiber

mats were darker as the CNT concentration increased (Figure 2C). Inclusion of densely localized CNTs within the PCL fibers was confirmed by transmission electron microscopy (Figure 2D). In general, conductivity improved with increasing CNT concentration, but 3% CNT-containing substrates were the most conductive, exhibiting an approximately 10× increase relative to the 1% CNT group (Figure 2E). It is likely that this drastic increase can be explained by an optimization between fiber diameter and CNT-derived conductivity. Electrical resistance is inversely proportional to cross-sectional area of the fibers, indicating that smaller fibers are more resistant to the flow of electrical current [28]. Therefore, moderately sized fibers containing 3% CNTs represented the best compromise between fiber diameter and CNT-derived conductivity, resulting in the most electrically conductive substrates.

The thermal characteristics resulting from varying the CNT loading concentrations were evaluated by differential scanning calorimetry (Figure 3). All curves had similar melting onsets and no significant difference was evident in the enthalpy of the samples; therefore, CNTs affect neither the onset of melting nor the enthalpy of the mixture (Figure 3A). In the cooling curves, nucleation and growth of PCL crystals were observed at a higher temperature in PCL 10% CNTs fibers than control (Figure 3B). This phenomenon represents heterogeneous nucleation [29]. CNTs are an effective nucleation site for PCL crystals, causing nucleation in PCL-CNT samples at lower undercooling than control. As in melting, the total enthalpy remains unchanged between the groups, indicating that the CNT activity in PCL is solely as a nucleating agent since no appreciable energy is measured related to chemical reactions. While CNTs do not affect the chemistry of PCL or its phase space, CNTs do affect the morphology of the crystals resulting in larger, more aligned crystal structures. The additional delay of crystalline onset in the control samples leads to smaller critical nuclei, a higher nucleation rate and a tendency to a more equiaxed distribution of crystals.

Cellular response with chemical treatment

Cells were cultured on PCL control or PCL 3% CNTs (PCL-CNTs) for all experiments in order to compare the effects of the least conductive and most conductive substrates, respectively. As a tissue culture control for the first set of experiments, cells were also cultured on TCPS.

We first evaluated changes in gene expression of cardiac markers for hMSCs cultured on TCPS, PCL or PCL-CNTs in the presence of either Aza or Jag in order to identify the role of each factor in modulating cardiomyogenic differentiation (Figure 4). Nkx2.5 is a transcription factor that appears early in cardiac differentiation and controls the regulation of several cardiac-specific genes [30]. α-MYH colocalizes with the actin cytoskeleton to generate contractile forces in cardiac tissue [31], and is known to be expressed at low basal levels in hMSCs [32]. cTNT is part of the troponin complex that has been used as a functional, late-stage marker of hMSC cardiac differentiation *in vivo* [33]. Ryanodine receptor 2 (RYR2) is an intracellular ion channel that releases Ca^{2+} from the sarcoplasmic reticulum to generate contractile forces in cardiac muscle [34].

For all genes of interest, hMSCs on PCL-CNTs under treatment with Aza exhibited the strongest level of expression when compared with all other groups (Figures 4A–4D). In general, Jag treatment did not enhance expression of cardiac genes on any of the three substrates. Interestingly, compared with PCL-CNT (+) Aza, expression of the early cardiac marker *Nkx2.5* was significantly lower for all groups except PCL (+) Aza (Figure 4A), indicating upregulation of early transcriptional activity in the presence of Aza on both polymer substrates.

We then sought to identify changes in cell morphology and actin/α-MYH colocalization between the most relevant groups as identified from the PCR results: PCL ± Aza versus PCL-CNT ± Aza (Figure 5). For hMSCs cultured on PCL scaffolds without Aza treatment, strong expression of α-MYH was observed, although it did not appear to colocalize well with filamentous (F)-actin cytoskeleton. Upon treatment with Aza on PCL scaffolds, α-MYH no longer appeared as continuous bands but rather became punctate and exhibited virtually no colocalization with the actin cytoskeleton. By contrast, hMSCs on the PCL-CNT substrate without Aza treatment assumed an elongated morphology similar to that of cardiomyocytes [35] with strong colocalization between α-MYH and F-actin cytoskeleton. It is worth noting that these substrates are 3D and the cells can potentially assume any morphology; since a rod-shaped, cardiomyocyte-like morphology was exhibited by default for hMSCs on PCL-CNT, it suggests that this substrate intrinsically possesses characteristics that encourage cardiac differentiation. Furthermore, upon treatment with Aza, hMSCs on the PCL-CNT substrates displayed extensive colocalization of the proteins of interest (Figure 5B, arrows). These data confirm that hMSCs cultured on PCL-CNT substrates in the presence of Aza exhibit the strongest degree of cardiomyogenic differentiation at both the gene and protein levels.

Electrical stimulation

After identifying the most effective chemical treatment group to enhance hMSC differentiation, we then added extrinsic ES to the system to evaluate the role of ES in further driving cardiac differentiation (Figures 6 & 7). Gene expression of cardiac markers was heavily influenced by ES and/or cotreatment with Aza and ES (Figures 6A–6D). Expression of the early cardiac marker *Nkx2.5* was significantly upregulated with cotreatment of Aza and ES on both substrates, but not with ES alone (Figure 6A). No clear trend was observed for the expression of late-stage markers at the gene level. Expression of α-*MYH* significantly decreased with ES or Aza + ES on PCL-CNT substrates compared with their control, but this effect was not observed on PCL alone (Figure 6B). In contrast, the opposite was observed for cTNT expression (Figure 6C). *RYR2* expression was significantly upregulated on PCL-CNT substrates with ES alone, but this effect was significantly reduced upon cotreatment with Aza (Figure 6D). This effect can likely be explained by the physiological role of *RYR2* through which calcium is released into the cytosol following stimulation by an electrical impulse [34].

In order to evaluate the protein- and cell-level influence of ES, we next observed changes in cell morphology and actin/α-MYH colocalization (Figure 7). For cells cultured on PCL substrates, ES improved colocalization of α-MYH and F-actin, as well as improved cell–cell contacts, but this enhancement was not observed on PCL-CNT substrates. Extrinsic ES appeared to severely downregulate α-MYH expression for hMSCs on PCL-CNTs, although cytoskeletal integrity persisted. ES did, however, alter the shape of hMSCs on PCL-CNT substrates, effectively inhibiting their cardiomyocyte-like, elongated morphology. Under cotreatment with ES and Aza, hMSCs on either substrate assumed severely altered morphologies with either no expression of α-MYH or a complete loss of protein colocalization.

Conclusion

Cardiac myocytes are electrically coupled through intermembrane and cell–cell ion channels and transporters, which allow for efficient electrical conduction of cardiac tissue and synchronized beating of the heart [10]. Our data indicate that composite scaffolds fabricated from biocompatible, nonconductive PCL embedded with electrically conductive CNTs can be used as synthetic cell culture platforms for enhanced differentiation of hMSCs. Through analysis of fiber morphology, elastic modulus and conductivity, we verified that scaffold

properties are affected by inclusion of CNTs and can be tailored for specific applications. In addition, we found that hMSCs cultured on 3D PCL-CNT substrates inherently assumed an elongated morphology with strong actin/α-MYH colocalization that suggested early cardiac differentiation. Although Jag protein did not affect hMSC differentiation, treatment with Aza was found to stimulate opposite effects in hMSCs, depending upon the substrate composition. Specifically, hMSCs on PCL substrates exhibited punctate expression of α-MYH in response to treatment with Aza, whereas hMSCs on PCL-CNT substrates demonstrated enhanced actin/α-MYH colocalization. Furthermore, extrinsically applied ES had divergent effects on hMSCs, depending upon the conductivity of the culture substrate. On the nonconductive PCL substrates, ES appeared to enhance cardiomyogenic differentiation of hMSCs at the protein and cell levels, but ES of cells on the conductive PCL-CNT substrates markedly decreased expression of the cardiac marker α-MYH. Cotreatment with ES and Aza severely reduced α-MYH expression on either substrate, indicating that the effects of the two stimuli are not synergistic. Therefore, our data show that early cardiac differentiation of hMSCs can be enhanced in two ways: by culturing cells on conductive, biocompatible PCL-CNT substrates without ES under treatment with Aza; or extrinsic ES on nonconductive PCL substrates without Aza treatment.

Because the functional consequences of the different treatment conditions were not evaluated in this study, future work will investigate the formation of syncitia and cell–cell gap junctions, as well as calcium handling dynamics, in order to verify physiologically relevant cardiomyogenic differentiation. In parallel, once *in vitro* predifferentiation protocols have been optimized, hMSCs will be locally delivered to the infarcted myocardium in an animal model to assess therapeutic activity *in vivo*. End point readouts for *in vivo* work will evaluate the integration of xenograft hMSCs with host tissue and expression profiles for transplantation-related cytokines (e.g., host response and inflammation).

Future perspective

Nanomaterial-mediated control over stem cell behavior is a novel field whose infancy is only now being realized. As the fields of cell biology, nanotechnology, medicine and materials science continue to advance in parallel, the applications of new knowledge and interdisciplinary collaborative efforts will undoubtedly pave the way for improved prevention, targeting and treatment of human diseases. In particular, the discovery of multipotent, tissue-specific stem cells coupled with improved techniques for designing and fabricating nanoscale materials provides a promising means for clinically translatable strategies aimed at regenerating lost or damaged tissue. Beyond the intrinsic need for improving patient care and disease management, these novel technologies must lend themselves to scalability to be rendered useful in the medical realm. Improving both our understanding and implementation of these novel materials is paramount to their success.

In the coming decade, the applications of nanomedicine toward deriving tissue-specific cell types for regenerative purposes will likely see drastic growth. Specifically, because heart disease and myocardial infarction are leading causes of death, nanotechnological techniques aimed at regenerating cardiac tissue will continue to gain interest, not only for the inherent gain in knowledge but also due to the lucrative financial promise. By mimicking the properties of biological tissues and elucidating the mechanisms by which stem cell differentiation occurs, nanomaterial approaches for driving stem cell behavior will continue to excite and challenge the scientists and engineers in our field.

Acknowledgments

The authors would like to acknowledge instrumental support (Enduratec Electroforce 3100 mechanical tester, Bose Corporation, MN, USA) from J Weis and MI Miga at Vanderbilt University (TN, USA).

References

Papers of special note have been highlighted as:

' of interest

'' of considerable interest

1''. Engler AJ, Sen S, Sweeney HL, Discher DE. Matrix elasticity directs stem cell lineage specification. Cell. 2006; 126(4):677–689. Material-mediated multilineage potential of human mesenchymal stem cells. [PubMed: 16923388]

2'. Wang X, Boire TC, Bronikowski CM, Zachman AL, Crowder SW, Sung HJ. Decoupling polymer properties to elucidate mechanisms governing cell behavior. Tissue Eng Part B Rev. 2012; 18(5): 396–404. A comprehensive overview regarding decoupling of polymer properties for elucidating cell responses. [PubMed: 22536977]

3. Martinelli V, Cellot G, Toma FM, et al. Carbon nanotubes promote growth and spontaneous electrical activity in cultured cardiac myocytes. Nano Lett. 2012; 12(4):1831–1838. [PubMed: 22432413]

4. Serena E, Figallo E, Tandon N, et al. Electrical stimulation of human embryonic stem cells: cardiac differentiation and the generation of reactive oxygen species. Exp Cell Res. 2009; 315(20):3611–3619. [PubMed: 19720058]

5. Dvir T, Timko BP, Brigham MD, et al. Nanowired three-dimensional cardiac patches. Nat Nanotechnol. 2011; 6(11):720–725. [PubMed: 21946708]

6. Kim DH, Provenzano PP, Smith CL, Levchenko A. Matrix nanotopography as a regulator of cell function. J Cell Biol. 2012; 197(3):351–360. [PubMed: 22547406]

7. Chen SS, Fitzgerald W, Zimmerberg J, Kleinman HK, Margolis L. Cell–cell and cell–extracellular matrix interactions regulate embryonic stem cell differentiation. Stem Cells. 2007; 25(3):553–561. [PubMed: 17332514]

8. Reilly GC, Engler AJ. Intrinsic extracellular matrix properties regulate stem cell differentiation. J Biomech. 2009; 43(1):55–62. [PubMed: 19800626]

9'. Povsic TJ, O'Connor CM. Cell therapy for heart failure: the need for a new therapeutic strategy. Expert Rev Cardiovasc Ther. 2010; 8(8):1107–1126. A strong review of the current strategies for treatment of heart complications, as well as their limitations. [PubMed: 20670189]

10. Wang F, Guan J. Cellular cardiomyoplasty and cardiac tissue engineering for myocardial therapy. Adv Drug Deliv Rev. 2010; 62(7–8):784–797. [PubMed: 20214939]

11. Horwitz EM, Gordon PL, Koo WK, et al. Isolated allogeneic bone marrow-derived mesenchymal cells engraft and stimulate growth in children with osteogenesis imperfecta: implications for cell therapy of bone. Proc Natl Acad Sci USA. 2002; 99(13):8932–8937. [PubMed: 12084934]

12. Nagaya N, Fujii T, Iwase T, et al. Intravenous administration of mesenchymal stem cells improves cardiac function in rats with acute myocardial infarction through angiogenesis and myogenesis. Am J Physiol Heart Circ Physiol. 2004; 287(6):H2670–H2676. [PubMed: 15284059]

13. Li H, Yu B, Zhang Y, Pan Z, Xu W. Jagged 1 protein enhances the differentiation of mesenchymal stem cells into cardiomyocytes. Biochem Biophys Res Commun. 2006; 341(2):320–325. [PubMed: 16413496]

14. Wakitani S, Saito T, Caplan AI. Myogenic cells derived from rat bone marrow mesenchymal stem cells exposed to 5-azacytidine. Muscle Nerve. 1995; 18(12):1417–1426. [PubMed: 7477065]

15. Xu W, Zhang X, Qian H, et al. Mesenchymal stem cells from adult human bone marrow differentiate into a cardiomyocyte phenotype *in vitro*. Exp Biol Med (Maywood). 2004; 229(7): 623–631. [PubMed: 15229356]

16. Giordano A, Galderisi U, Marino IR. From the laboratory bench to the patient's bedside: an update on clinical trials with mesenchymal stem cells. J Cell Physiol. 2007; 211(1):27–35. [PubMed: 17226788]

17''. Perin EC, Willerson JT, Pepine CJ, et al. Effect of transendocardial delivery of autologous bone marrow mononuclear cells on functional capacity, left ventricular function, and perfusion in chronic heart failure: the FOCUS-CCTRN trial. JAMA. 2012; 307(16):1717–1726. Results of a 6-month clinical trial regarding the use of autologous mesenchymal cells to treat cardiac dysfunction. [PubMed: 22447880]

18'. Mooney E, Dockery P, Greiser U, Murphy M, Barron V. Carbon nanotubes and mesenchymal stem cells: biocompatibility, proliferation and differentiation. Nano Lett. 2008; 8(8):2137–2143. A brief but informative overview for how carbon nanotubes interact with mesenchymal stem cells. [PubMed: 18624387]

19. Meng X, Stout DA, Sun L, Beingessner RL, Fenniri H, Webster TJ. Novel injectable biomimetic hydrogels with carbon nanofibers and self assembled rosette nanotubes for myocardial applications. J Biomed Mater Res A. 2012; 101(4):1095–1102. [PubMed: 23008178]

20. Mooney E, Mackle JN, Blond DJ, et al. The electrical stimulation of carbon nanotubes to provide a cardiomimetic cue to MSCs. Biomaterials. 2012; 33(26):6132–6139. [PubMed: 22681974]

21. Lee HH, Shin US, Jin GZ, Kim HW. Highly homogeneous carbon nanotube–polycaprolactone composites with various and controllable concentrations of ionically-modified-MWCNTs. Bull Korean Chem Soc. 2011; 32(1):157–161.

22. Gupta MK, Walthall JM, Venkataraman R, et al. Combinatorial polymer electrospun matrices promote physiologically-relevant cardiomyogenic stem cell differentiation. PLoS ONE. 2011; 6(12):e28935. [PubMed: 22216144]

23. Crowder SW, Gupta MK, Hofmeister LH, Zachman AL, Sung HJ. Modular polymer design to regulate phenotype and oxidative response of human coronary artery cells for potential stent coating applications. Acta Biomater. 2012; 8(2):559–569. [PubMed: 22019760]

24. Christopherson GT, Song H, Mao HQ. The influence of fiber diameter of electrospun substrates on neural stem cell differentiation and proliferation. Biomaterials. 2009; 30(4):556–564. [PubMed: 18977025]

25. Bianco A, Del Gaudio C, Baiguera S, et al. Microstructure and cytocompatibility of electrospun nanocomposites based on poly(epsilon-caprolactone) and carbon nanostructures. Int J Artif Organs. 2010; 33(5):271–282. [PubMed: 20593348]

26. Clark MD, Krishnamoorti R. Dispersion of functionalized multiwalled carbon nanotubes. J Phys Chem C. 2009; 113(49):20861–20868.

27. Saeed K, Park SY, Lee HJ, Baek JB, Huh WS. Preparation of electrospun nanofibers of carbon nanotube/polycaprolactone nanocomposite. Polymer. 2006; 47(23):8019–8025.

28. Purcell, EM. Electricity and Magnetism. McGraw-Hill; Newton, MA, USA: 1985. p. 2

29. Turnbull D. Kinetics of heterogeneous nucleation. J Chem Phys. 1950; 18(2):198–203.

30. Qian Q, Qian H, Zhang X, et al. 5-azacytidine induces cardiac differentiation of human umbilical cord-derived mesenchymal stem cells by activating extracellular regulated kinase. Stem Cells Dev. 2011; 21(1):67–75. [PubMed: 21476855]

31. Ng WA, Grupp IL, Subramaniam A, Robbins J. Cardiac myosin heavy chain mRNA expression and myocardial function in the mouse heart. Circ Res. 1991; 68(6):1742–1750. [PubMed: 2036722]

32. Bayes-Genis A, Roura S, Soler-Botija C, et al. Identification of cardiomyogenic lineage markers in untreated human bone marrow-derived mesenchymal stem cells. Transplant Proc. 2005; 37(9): 4077–4079. [PubMed: 16386630]

33. Toma C, Pittenger MF, Cahill KS, Byrne BJ, Kessler PD. Human mesenchymal stem cells differentiate to a cardiomyocyte phenotype in the adult murine heart. Circulation. 2002; 105(1): 93–98. [PubMed: 11772882]

34. Sorrentino V, Volpe P. Ryanodine receptors: how many, where and why? Trends Pharmacol Sci. 1993; 14(3):98–103. [PubMed: 8387707]

35. Kang PM, Haunstetter A, Aoki H, Usheva A, Izumo S. Morphological and molecular characterization of adult cardiomyocyte apoptosis during hypoxia and reoxygenation. Circ Res. 2000; 87(2):118–125. [PubMed: 10903995]

Executive summary

Background

- Human mesenchymal stem cells (hMSCs) are a promising cell source for regenerating lost or damaged cardiac tissue.
- Electrically active synthetic substrates have been employed in previous studies for the maintenance and/or formation of cardiac tissue.

Materials & methods

- Composite electrospun scaffolds of poly(ε-caprolactone) (PCL) and multiwall carbon nanotubes (CNTs) were generated by electrospinning.

Results & discussion

- By altering the loading concentration of CNTs, the properties of the fiber mats could be tailored, including fiber diameter, elastic modulus and electrical conductivity.
- A mixture of 3% w/w CNTs to PCL was shown to produce the most electrically conductive substrates, and these were used for cell culture studies against the nonconductive PCL control.
- When cultured upon electrically conductive PCL-CNT substrates, hMSCs assumed a cardiomyocyte-like phenotype, and this effect was further enhanced under treatment with the epigenetic regulator, 5-azacytidine, both at the gene and protein levels.
- Extrinsic electrical stimulation was shown to enhance cardiomyogenic differentiation of hMSCs at the protein level when cultured in PCL substrates, but this effect was not observed for electrically conductive PCL-CNT substrates.
- This study provides novel insight for driving cardiomyogenic differentiation of hMSCs for regenerating damaged cardiac tissue.

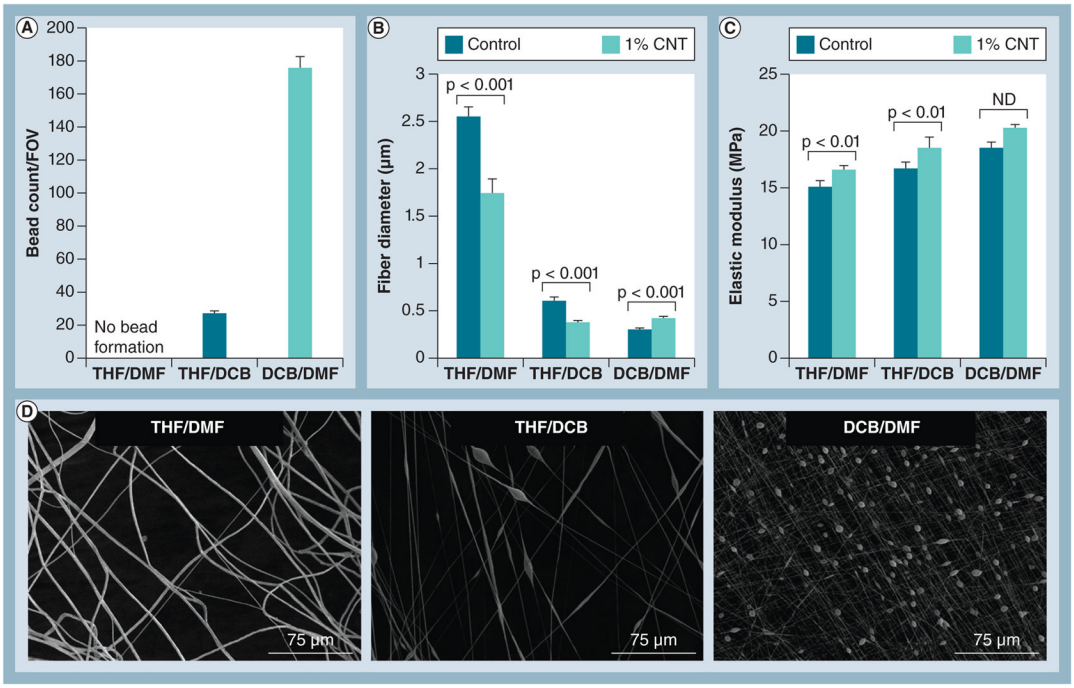

Figure 1. Selection of electrospinning solvents

(A) Bead formation in each FOV and **(B)** fiber diameter of poly(ε-caprolactone) (control with no CNT inclusion) are affected by solvent groups as well as inclusion of 1% CNTs. **(C)** Elastic modulus was within the same range for control fibers from all solvent groups, but increased with the addition of 1% CNTs (n = 9 samples/group). **(D)** Representative scanning electron microscopy images showing differences in bead formation and fiber diameter for control fibers from the different solvent groups.

CNT: Carbon nanotube; DCB: Dichlorobenzene; DMF: Dimethylformamide; FOV: Field of view; ND: No statistical difference; THF: Tetrahydrofuran.

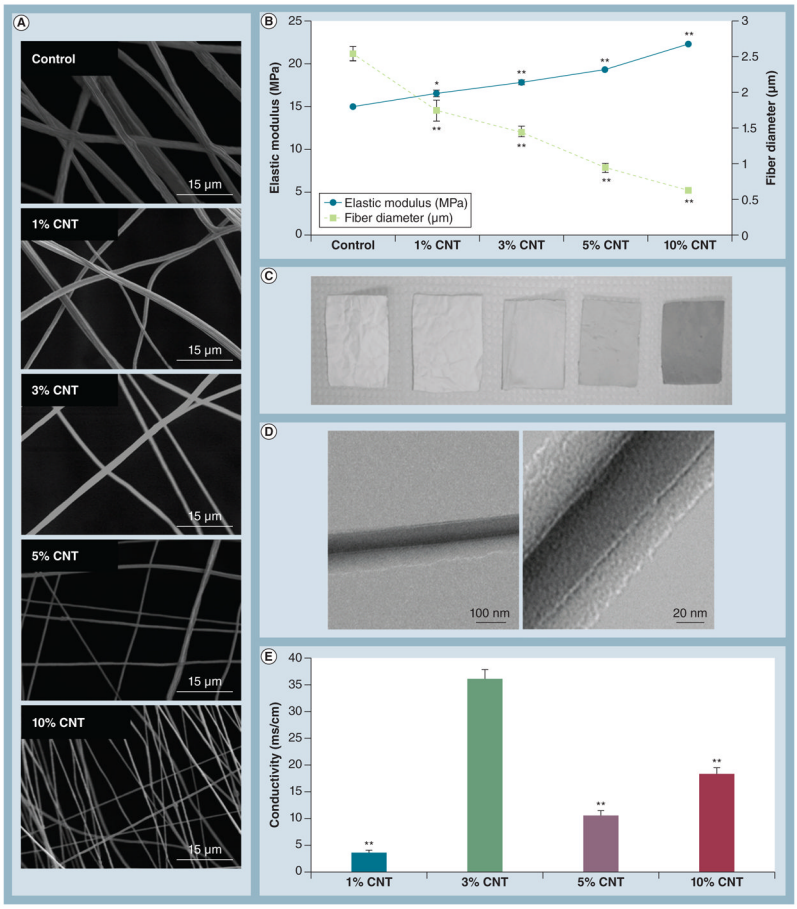

Figure 2. Optimization of carbon nanotube loading concentration

(A) Representative scanning electron microscopy images of mats spun for 20 min demonstrated a decrease in fiber diameter with increasing CNT loading concentration. **(B)** An inverse correlation between elastic modulus and fiber diameter was observed with increasing CNT concentration (n = 9 samples/group for elastic modulus). *p < 0.05 and **p < 0.001 versus control. **(C)** Fiber mats containing higher CNT concentrations were markedly darker, indicating successful incorporation of CNTs. **(D)** Representative images of CNTs embedded within polymer fibers by transmission electron microscopy for the 5%CNT group. **(E)** Overall, electrical conductivity correlated with CNT concentration except for mats containing 3% CNTs, which exhibited excellent conductivity (n = 3 samples/group). **p < 0.01 versus 3%CNT.

CNT: Carbon nanotube.

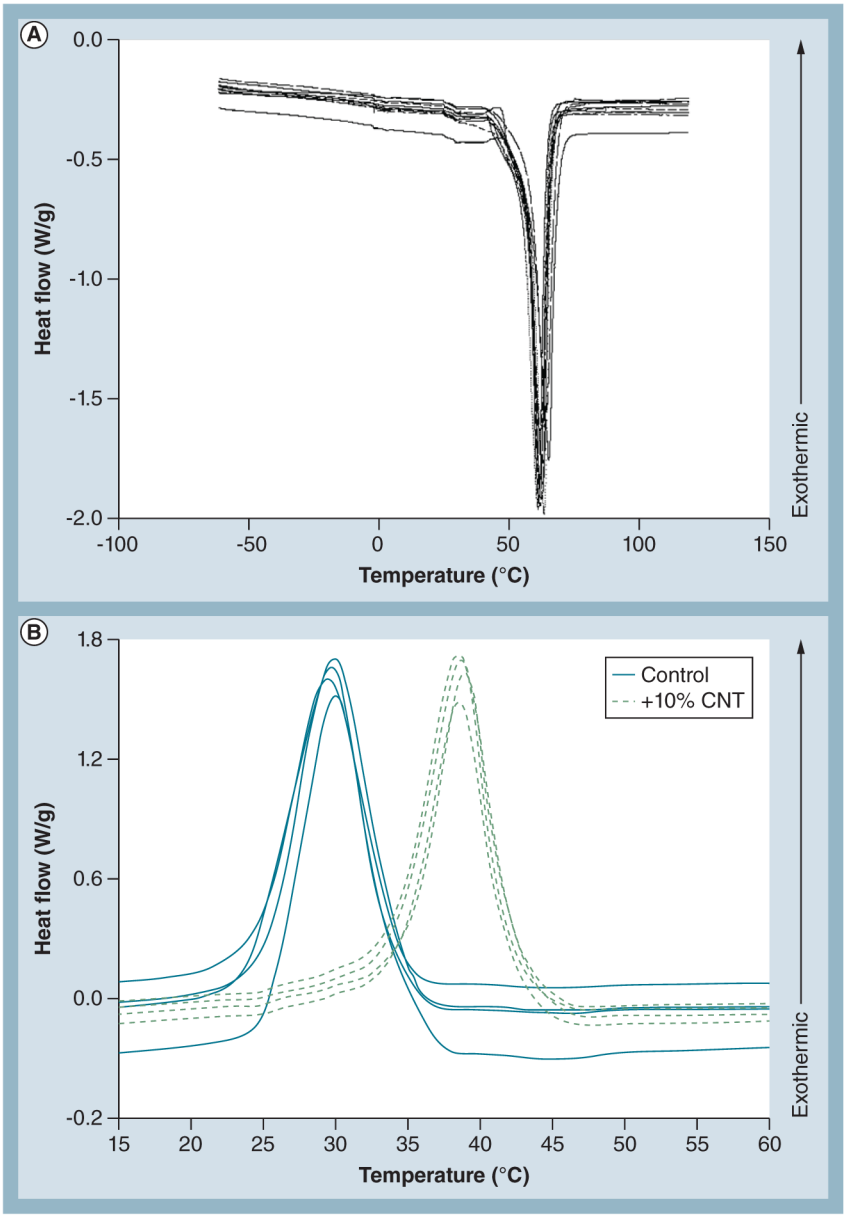

Figure 3. Thermal properties of carbon nanotube loading groups

(A) Differential scanning calorimetry reveals that melting temperature is not affected by CNT loading concentration (n = 2 representative curves/group, totaling ten curves). Curves are not labeled because they could not be distinguished due to the tight distribution. **(B)** Differential scanning calorimetry demonstrated that CNTs heavily influenced the crystallization temperature and cooling kinetics of the samples (n = 4 representative curves/group, totaling eight curves). The cooling curves reveal heterogeneous nucleation in the 10% CNT-containing samples. CNTs acted as a nucleation site in the samples, forming poly(ε-caprolactone) (PCL) crystals at a higher temperature compared with PCL alone. This resulted in more tightly packed PCL crystals in the CNT-containing groups.
CNT: Carbon nanotube.

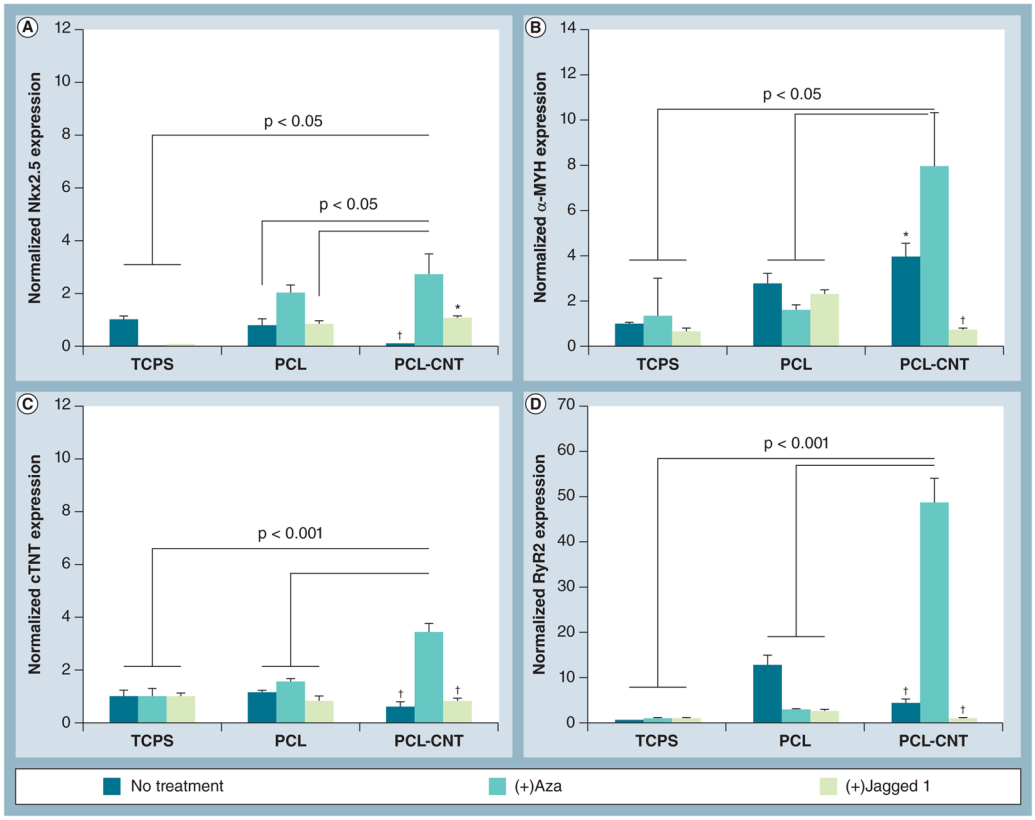

Figure 4. Gene expression of cardiac markers by human mesenchymal stem cells under chemical treatment

Reverse transcriptase-PCR analyses following 8-day *in vitro* culture of human mesenchymal stem cells on PCL or PCL-CNT substrates. **(A)** Nkx2.5, an early marker of cardiac differentiation, and late-stage cardiac markers **(B)** α-MYH, **(C)** cTNT and **(D)** RyR2 were all significantly upregulated on PCL-CNT substrates under treatment with Aza. Treatment with Jagged 1 protein did not appear to significantly affect gene expression. All groups were normalized to glyceraldehyde 3-phosphate dehydrogenase expression (reference control) as well as TCPS no treatment sample (sample control) because TCPS is the classical method by which human mesenchymal stem cells are normally cultured. Lines represent statistical significance between PCL-CNT + Aza versus groups indicated by lines.

*$p < 0.05$, †$p < 0.01$ versus PCL-CNT + Aza.

α-MYH: α-myosin heavy chain; Aza: 5-azacytidine; CNT: Carbon nanotube; cTNT: Cardiac troponin T; PCL: Poly(ε-caprolactone); RyR2: Ryanodine receptor 2; TCPS: Tissue culture polystyrene.

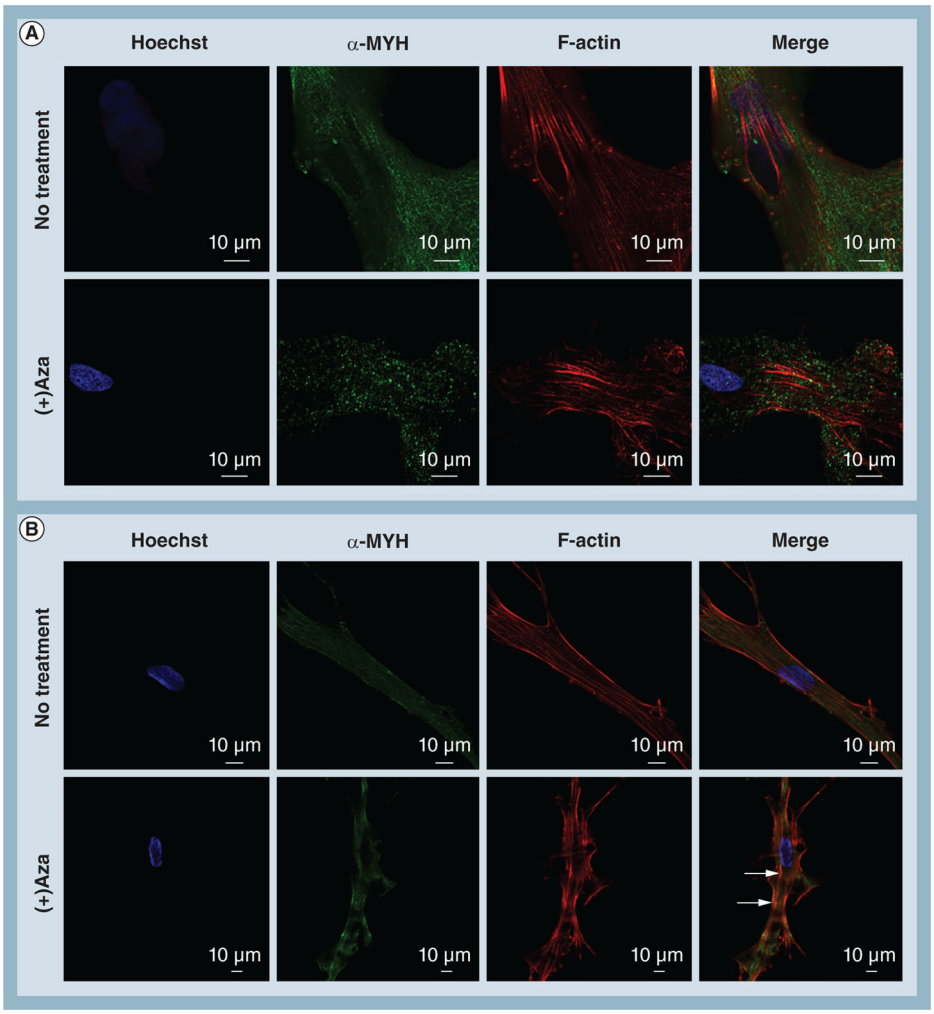

Figure 5. Confocal imaging of intracellular protein localization and cell morphology of human mesenchymal stem cells under 5-azacytidine treatment. (A)
Human mesenchymal stem cells on poly(ε-caprolactone) without treatment exhibited strong expression of α-MYH that was partially localized with F-actin. Under treatment with Aza, α-MYH expression became punctate and lost all colocalization with F-actin. **(B)** In contrast, human mesenchymal stem cells on poly(ε-caprolactone) carbon nanotube substrates assumed an elongated morphology that resembled rod-shaped cardiomyocytes. In addition, moderate colocalization of α-MYH bands with F-actin was observed. Under Aza treatment, this colocalization (arrows) was further enhanced, indicating strong differentiation towards a cardiomyogenic lineage.
α-MYH: α-myosin heavy chain; Aza: 5-azacytidine; F-actin: Filamentous actin.

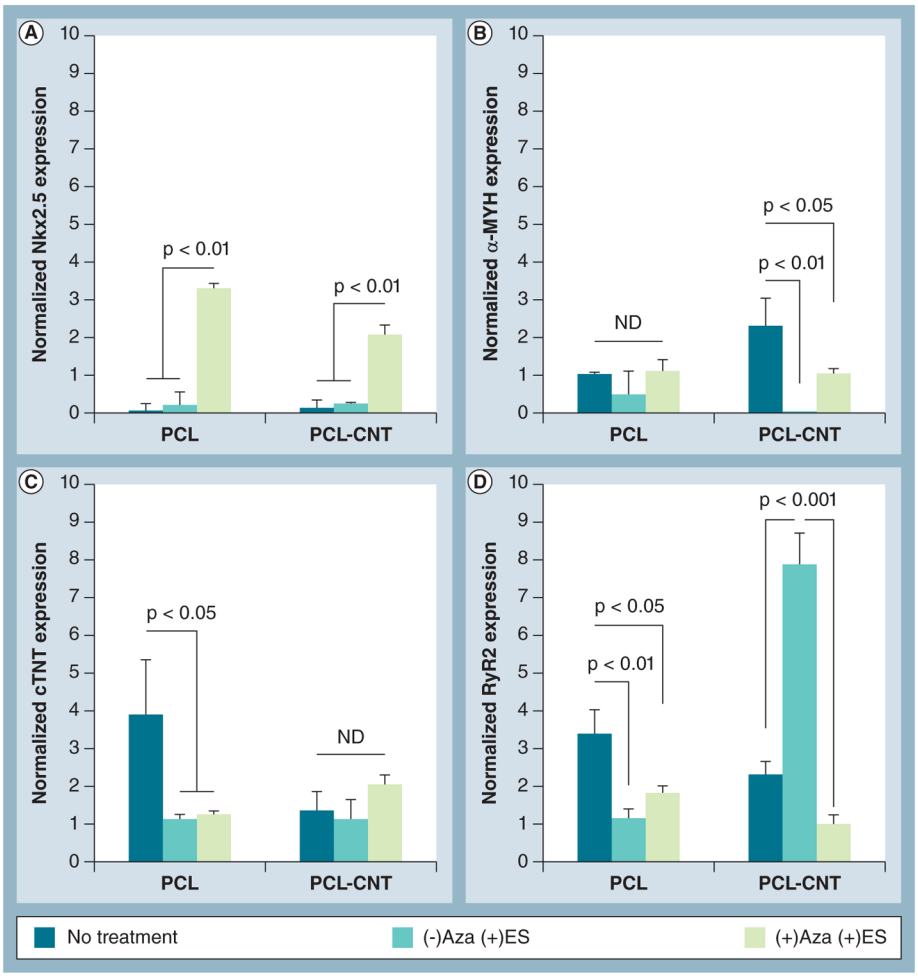

Figure 6. Gene expression of cardiac markers by human mesenchymal stem cells in response to extrinsic electrical stimulation

Human mesenchymal stem cells cultured on PCL or PCL-CNT substrates were paced with electrical stimulation for 10 min/day for 4 days prior to end point reverse transcriptase-PCR analyses. Gene expression of the cardiac markers **(A)** Nkx2.5, **(B)** α-myosin heavy chain, **(C)** cardiac troponin T and **(D)** ryanodine receptor 2 showed no clear trend in response to ES ± Aza treatment. All groups were normalized to glyceraldehyde 3-phosphate dehydrogenase expression (reference control) but no sample control was used since tissue culture polystyrene was not included in this portion of the study. Lines indicate statistical significance between groups.

Aza: 5-azacytidine; CNT: Carbon nanotube; ES: Electrical stimulation; ND: No statistical difference; PCL: Poly(ε-caprolactone).

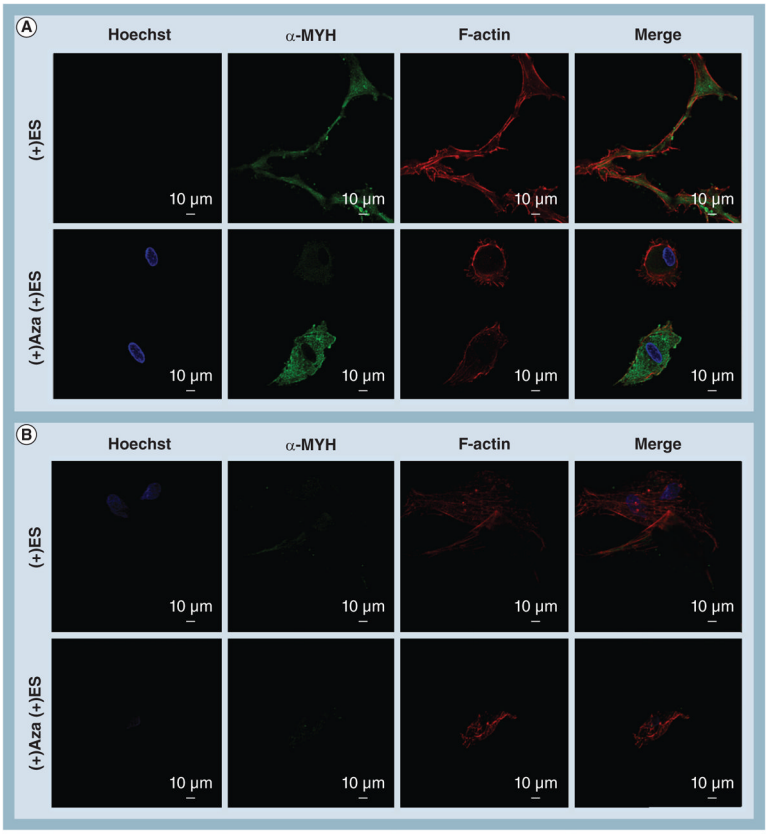

Figure 7. Confocal imaging of human mesenchymal stem cell protein localization and cell morphology following electrical stimulation

(A) In the presence of ES, human mesenchymal stem cells cultured on poly(ε-caprolactone) substrates increased cell–cell contacts with neighboring cells and maintained strong expression of α-MYH as well as colocalization with F-actin. **(B)** In contrast, ES completely silenced expression of α-MYH for human mesenchymal stem cells on poly(ε-caprolactone) carbon nanotube substrates and caused cells to lose their elongated morphology. For cells cultured on either substrate, cotreatment with ES and Aza resulted in a complete deregulation of normal cell function as indicated by changes in cell morphology and either loss of α-MYH expression or colocalization with actin.

α-MYH: α-myosin heavy chain; Aza: Azacytidine; ES: Electrical stimulation; F-actin: Filamentous actin.